Positive Dendritic Effect in DNA/Porphyrin Composite Photocurrent Generators Containing Dendrimers as the Stationary Phase

Shin Ogasawara, Atsushi Ikeda,* and Jun-ichi Kikuchi

Graduate School of Materials Science, Nara Institute of Science and Technology, Takayama, Ikoma, Nara 630-0192, Japan.

Received August 1, 2006. Revised Manuscript Received October 7, 2006

In this study, we used PAMAM dendrimers (**G1**−**G4**) as stationary phases to deposit porphyrin-intercalated DNA onto ITO electrodes. The surface density of the external amino moieties of the dendrimers, i.e., the cationic charge density on the surface, increased with each generation, and correspondingly increased the surface coverage of DNA and porphyrin (**1**) units through electrostatic interactions and intercalation. The resulting dendrimer−DNA−**1** membranes were sufficiently stable that they did not peel off the ITO electrodes. The resulting electrodes generated photocurrent waves in response to irradiation with visible light. The photocurrent increased exponentially upon increasing the generation of the dendrimer, i.e., we observed a positive dendritic effect in these systems; actually, the photocurrent for the **G4**−DNA−**1** membrane (77.5 nA cm^{-2} at 440 nm) was ca. nine times larger than that for the **G1**−DNA−**1** membrane (8.5 nA cm^{-2} at 440 nm), and the quantum yield for the former (1.0%) was five times larger than that for the latter (0.2%). Furthermore, the performance of the two-dimensional polymer **G4** as a stationary phase was far superior to that of the one-dimensional polymer poly(allylamine hydrochloride) (**PAH**).

Introduction

Organic photocurrent generators consisting of electron-donors or acceptors have provoked a great deal of interest in the development of photovoltaic devices.[1−5] Indeed, many groups have reported the development of photocurrent generators using Langmuir−Blodgett (LB)[2] membranes and self-assembled monolayers (SAMs).[3] Using these approaches, monolayer systems comprising covalently linked donor−acceptor molecules can provide excellent light-to-current conversion yields.[3−5] Unfortunately, synthetic difficulties arise when covalently linking the thin-layer-forming substituents, the donor units, and the acceptor units into one molecular system. We have investigated several general methods for using electrostatic interactions to develop photocurrent generator systems on the electrode.[4,6,7] Among these approaches, the use of Nafion as a supporting matrix allowed for the deposition of small donor−acceptor molecules on electrodes, without the need to chemically modify the donor−acceptor molecules, through electrostatic interactions.[7] In particular, we found that Nafion membranes could be used as stationary phases to deposit 5,10,15,20-tetrakis-(1-methyl-4-pyridinio)porphyrin tetrakis(*p*-toluenesulfonate) (TMPyP, **1**) onto an indium tin oxide (ITO) electrode. The resulting Nafion−**1** membrane was stable and did not peel off the ITO electrode because Nafion is only slightly soluble in water. In that system, a photocurrent was generated in response to irradiation with visible light (quantum yield: 3.5%). However, the microenvironments of porphyrin **1** in Nafion could not be determined. The reason for using DNA as a dye matrix for depositing **1** through electrostatic interactions and intercalation on an electrode are: (1) although a small molecule such as 5,10,15,20-tetrakis(4-sulfonatophenyl)-21*H*,23*H*-porphine, sodium salt (TPPS) was deposited directly on the ITO electrode covered with the cationic PAMAM dendrimers, it is easily peeled off the ITO

* Corresponding author. Fax: 81-0743-72-6099. Tel: 81-0743-72-6091. E-mail: aikeda@ms.naist.jp.

(1) (a) O'Regan, B.; Grätzel, M. *Nature* **1991**, *353*, 737−740. (b) Yu, G.; Gao, J.; Hummelen, J. C.; Wudl, F.; Heeger, A. J. *Science* **1995**, *270*, 1789−1791. (c) Kymakis, E.; Amaratunga, G. A. J. *Sol. Energy Mater. Sol. Cells* **2003**, *80*, 465−472. (d) Sharma, G. D.; Sharma, S. K.; Roy, M. S. *Mater. Sci. Eng., B* **2003**, *100*, 13−17. (e) Li, H.; Li, Y.; Zhai, J.; Cui, G.; Liu, H.; Xiao, S.; Liu, Y.; Lu, F.; Jiang, L.; Zhu, D. *Chem.*−*Eur. J.* **2003**, *9*, 6031−6038.

(2) (a) Fujihira, M. *Mol. Cryst. Liq. Cryst.* **1990**, *183*, 59−69. (b) Fujihira, M.; Nishiyama, K.; Yamada, H. *Thin Solid Films* **1985**, *132*, 77−82. (c) Zhang, W.; Shi, Y.; L.; Wu, Gan, N.; Huang, C.; Wu, D. *Langmuir* **1999**, *15*, 6921−6924.

(3) (a) Kondo, T.; Ito, T.; Nomura, S.; Uosaki, K. *Thin Solid Films* **1996**, *284/285*, 652−655. (b) Uosaki, K.; Kondo, T.; Zhang, X.-Q.; Yanagida, M. *J. Am. Chem. Soc.* **1997**, *119*, 8367−8368. (c) Imahori, H.; Yamada, H.; Ozawa, S.; Ushida, K.; Sakata, Y. *Chem. Commun.* **1999**, 1165−1166. (d) Imahori, H.; Yamada, H.; Nishimura, Y.; Yamazaki, I.; Sakata, Y. *J. Phys. Chem. B* **2000**, *104*, 2099−2108. (e) Imahori, H.; Norieda, H.; Yamada, H.; Nishimura, Y.; Yamazaki, I.; Sakata, Y.; Fukuzumi, S. *J. Am. Chem. Soc.* **2001**, *123*, 100−110. (f) Hirayama, D.; Takimiya, K.; Aso, Y.; Otsubo, T.; Hasobe, T.; Yamada, H.; Imahori, H.; Fukuzumi, S.; Sakata, Y. *J. Am. Chem. Soc.* **2002**, *124*, 532−533.

(4) (a) Hatano, T.; Ikeda, A.; Sano, M.; Kanekiyo, Y.; Shinkai, S. *J. Chem. Soc., Perkin Trans.* **2000**, *2*, 909−912. (b) Ikeda, A.; Hatano, T.; Shinkai, S.; Akiyama, T.; Yamada, S. *J. Am. Chem. Soc.* **2001**, *123*, 4855−4856. (c) Ikeda, A.; Hatano, T.; Konishi, T.; Shinkai, S. *Tetrahedron* **2003**, *59*, 3537−3540.

(5) Luo, C. P.; Guldi, D. M.; Maggini, M.; Menna, E.; Mondini, S.; Kotov, N. A.; Prato, M. *Angew. Chem., Int. Ed.* **2000**, *39*, 3905−3909.

(6) (a) Hatano, T.; Takeuchi, M.; Ikeda, A.; Shinkai, S. *Chem. Commun.* **2003**, 342−343. (b) Hatano, T.; Bae, A.-H.; Sugiyasu, K.; Fujita, N.; Takeuchi, M.; Ikeda, A.; Shinkai, S. *Org. Biomol. Chem.* **2003**, *1*, 2343−2347.

(7) (a) Tsuchiya, Y.; Ikeda, A.; Konishi, T.; Kikuchi, J. *J. Mater. Chem.* **2004**, *14*, 1128−1131. (b) Ikeda, A.; Tsuchiya, Y.; Konishi, T.; Ogasawara, S.; Kikuchi, J. *Chem. Mater.* **2005**, *17*, 4018−4022.

10.1021/cm061812i CCC: $33.50
Published on Web 11/16/2006

electrode in an electrolyte solution;[8] (2) the structure of porphyrin **1** in DNA is already known;[9] and (3) it is of interest from both photophysical and biochemical points of view.[9] Unfortunately, DNA deposits poorly on a 2-aminoethanethiol hydrochloride-covered ITO electrode, i.e., a surface that possess cationic charge. Therefore, to prevent exfoliation of a "water-soluble" DNA membrane, we have employed cationic poly(amideamine) (PAMAM) dendrimers[10] as stationary phases between anionic DNA and electrodes having an anionic surface charge. Despite the fact that dendrimers, which are monodisperse hyperbranched polymers, continue to attract a great deal of attention, very few positive dendritic effects have been reported.[11] This paper presents a novel photocurrent generator based on a dendrimer−DNA−**1** membrane that was stabilized through electrostatic interactions; for this system, we observed a positive dendritic effect on the photocurrent density.

Results and Discussion

Surface Coverage of Dendrimers and DNA. We used QCM to quantitatively characterize the formation of the dendrimers−DNA−**1** composite films. The frequency changes ($-\Delta F$) of 10.3, 19.7, 28.7, and 42.7 Hz for **G1**, **G2**, **G3**, and **G4** (see Chart 1) translate into surface coverages of 7.2×10^{-12}, 6.0×10^{-12}, 4.2×10^{-12}, and 3.0×10^{-12} mol cm^{-2}, respectively (Figure 1a and the Supporting Information, Table S1).[12] These results indicate that the surface coverage decreased upon increasing the generation of the dendrimers. In contrast, the surface density of the external amino moieties of the dendrimers, i.e., the charge density on the surface, increased with each generation (**G1**, 1.0×10^{-10}; **G2**, 1.8×10^{-10}; **G3**, 2.6×10^{-10}; and **G4**, 3.8×10^{-10} mol cm^{-2}; Figure 1a and the Supporting Information, Table S1). We attribute this phenomenon to (a) increased stabilization through multipoint interactions of the dendrimers with the electrode surfaces and (b) decreased electrostatic repulsion resulting from the reduced surface area per amino moiety for the higher-generation dendrimers. We estimated the surface coverages of DNA for the **G1**−DNA, **G2**−DNA, **G3**−DNA, and **G4**−DNA systems to be 1.0×10^{-10}, 2.0×10^{-10}, 2.8×10^{-10}, and 3.1×10^{-10} mol cm^{-2}, respectively, in terms of the abundance of nucleotide phosphate (NP); these values coincide well with the surface densities of external amino moieties of the dendrimers (Figure 1b and the Supporting Information, Table S2). This result indicates that the cationic charge density of the dendrimer determined the surface coverage of DNA; i.e., the cationic charge density on the surface decreased in the order **G4** > **G3** > **G2** > **G1**, and the adsorption of anionic DNA chains followed accordingly. We could not determine the surface coverage of **1** through QCM measurements because the resulting data were greater than the limits of the experimental error, for reasons that remain unclear to us.

Surface Coverage of 1. We measured the UV−vis absorption spectra of the electrodes coated with **G1**−DNA−**1**, **G2**−DNA−**1**, **G3**−DNA−**1**, and **G4**−DNA−**1** to determine the surface coverages of **1** (Figure 2). Each electrode exhibited an absorption maximum at 436 nm, which corresponds to the Soret band of the porphyrin intercalated into DNA.[9] From the known molar absorption coefficient ($\epsilon_{436} = 7.34 \times 10^8$ M^{-1} cm^{-1}) for **1** intercalated into DNA,[13] we estimated the surface coverages of **1** in the **G1**−DNA−**1**, **G2**−DNA−**1**, **G3**−DNA−**1**, and **G4**−DNA−**1** membranes to be 1.4×10^{-11}, 1.9×10^{-11}, 2.3×10^{-11}, and 2.6×10^{-11} mol cm^{-2}, respectively (Figure 1c and the Supporting Information, Table S3).[14,15] These surface coverages for **1** correlate well with those of DNA.

Photocurrent Generation. We observed the appearance of photocurrent waves (77.5 nA cm^{-2}; Figure 3) when the ITO electrode covered with the **G4**−DNA−**1** complex was irradiated with 440 nm light at a bias voltage of 0.4 V. The photoresponsive phenomena were repeated reversibly many times, indicating that the external amino moieties of the dendrimer did not act as a sacrificial reagent; further evidence supporting this concept is described below. We believe that the photoexcitation energy of **1** was transferred to the ITO electrode because the action spectrum was comparable with the UV−vis spectrum of the **G4**−DNA−**1** membrane (Figure 4).

Dendritic Effect for Photocurrent. We examined the influence that the generation of the dendrimer has on the values of the photocurrents and quantum yields. Figure 5 presents that the action spectra, recorded between 400 and 600 nm, for the **G1**−DNA−**1**, **G2**−DNA−**1**, **G3**−DNA−**1**, and **G4**−DNA−**1** systems. It is clear from the inset of Figure 5 that the photocurrent densities at 440 nm did not increase linearly in proportion to the surface coverage of **1**, but instead increased exponentially with respect to the generation of the dendrimer (8.5, 14.9, 26.9, and 77.5 nA

(8) Our preliminary experiments show that a small molecule such as TPPS was able to be deposited directly on the ITO electrode covered with the cationic PAMAM dendrimers. The surface coverage of TPPS was about four times greater than that of **G4**−DNA−**1** membrane. However, it was easily peeled off the ITO electrode in an electrolyte solution.

(9) (a) Gu, J.; Cai, L.; Tanaka, S.; Otsuka, Y.; Tabata, H.; Kawai, T. *J. Appl. Phys.* **2002**, *92*, 2816−2820. (b) Gu, J.; Tanaka, S.; Otsuka, Y.; Tabata, H.; Kawai, T. *Appl. Phys. Lett.* **2002**, *80*, 688−690. (c) Okahata, Y.; Kobayashi, T.; Tanaka, K.; Shimomura, M. *J. Am. Chem. Soc.* **1998**, *120*, 6165−6166.

(10) (a) Tomalia, D. A.; Baker, H.; Dewald, J. R.; Hall, M.; Kallos, G.; Martin, S.; Roeck, J.; Ryder, J.; Smith, P. *Macromolecules* **1986**, *19*, 2466−2468. (b) Zeng, F.; Zimmerman, S. C. *Chem. Rev.* **1997**, *97*, 1681−1712. (c) Bosman, A. W.; Janssen, H. M.; Meijer, E. W. *Chem. Rev.* **1999**, *99*, 1665−1688.

(11) (a) Valério, C.; Fillaut, J.-L.; Ruiz, J.; Guittard, J.; Blais, J.-C.; Astruc, D. *J. Am. Chem. Soc.* **1997**, *119*, 2588−2589. (b) Fan, Q.-H.; Chen, Y.-M.; Chen, X.-M.; Jiang, D.-Z.; Xi F.; Chan, A. S. C. *Chem. Commun.* **2000**, 789−790. (c) Ooe, M.; Murata, M.; Mizugaki, T.; Ebitani, K.; Kaneda, K. *J. Am. Chem. Soc.* **2004**, *126*, 1604−1605. (d) Numata, M.; Ikeda, A.; Fukuhara, C.; Shinkai, S. *Tetrahedron Lett.* **1999**, *40*, 6945−6948.

(12) Katagiri, K.; Hamasaki, R.; Ariga, K.; Kikuchi, J. *Langmuir* **2002**, *18*, 6709−6711.

(13) Bae, A.-H.; Hatano, T.; Sugiyasu, K.; Kishida, T.; Takeuchi, M.; Shinkai, S. *Tetrahedron Lett.* **2005**, *46*, 3169−3173.

(14) We also obtained a cyclic voltammogram (CV) of the deposited ITO electrode to provide further evidence of the deposition of **1**. Unfortunately, because the electron-transfer between the ITO electrode and **1** occurred only at a part of the membrane close to the electrode surface, we could not accurately compute the surface concentration of **1** from its oxidation peak area.

(15) Uosaki, et al., have also determined the concentration of a porphyrin from its absorption, see: Shimazu, K.; Takechi, M.; Fujii, H.; Suzuki, M.; Saiki, H.; Yoshimura, T.; Uosaki, K. *Thin Solid Films* **1996**, *273*, 250−253.

Chart 1

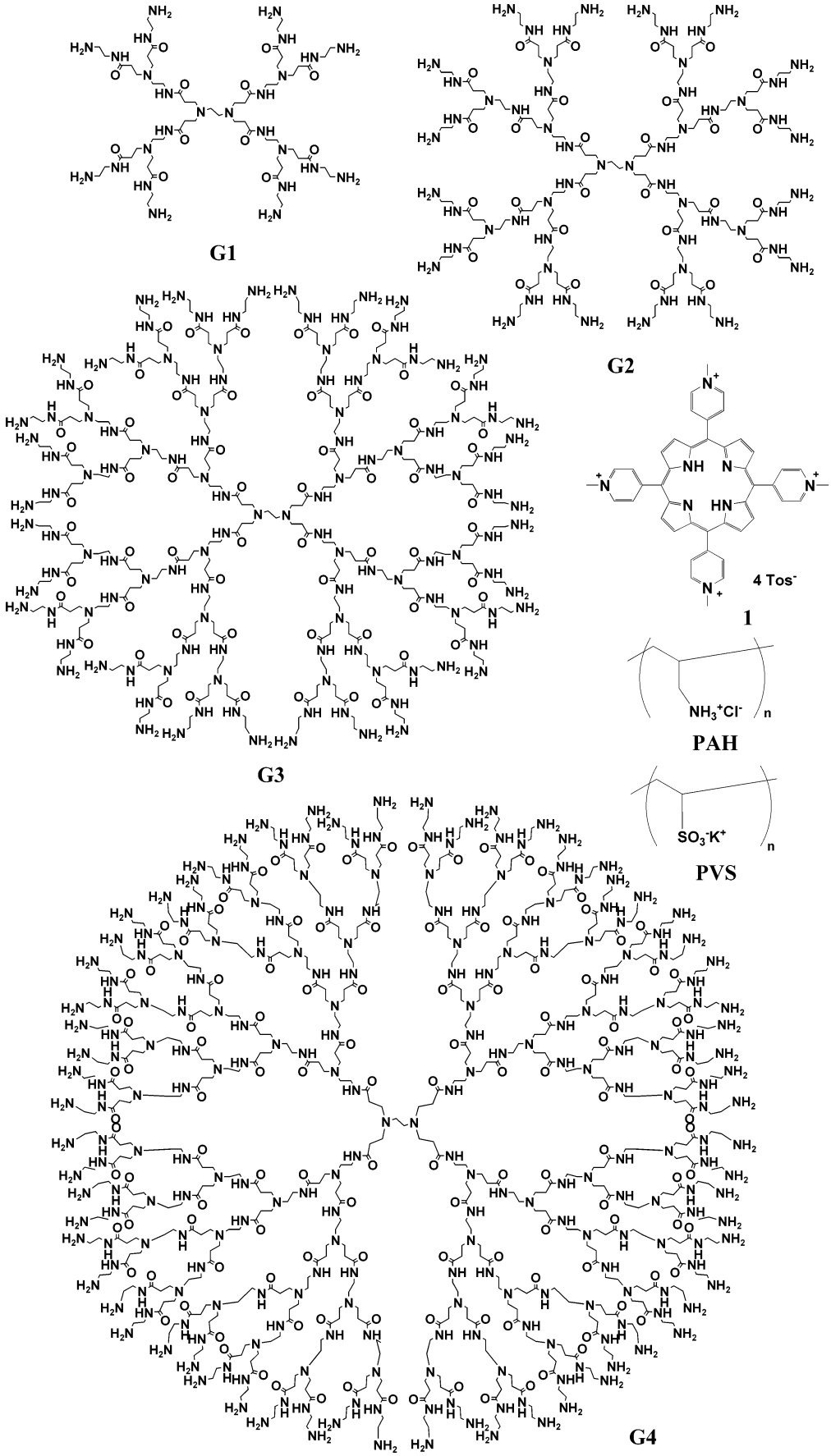

cm^{-2} for **G1**, **G2**, **G3**, and **G4**, respectively; see the Supporting Information, Table S4), indicating that this system exhibits a positive dendritic effect. These results were unexpected; we believe that the photocurrents would decrease

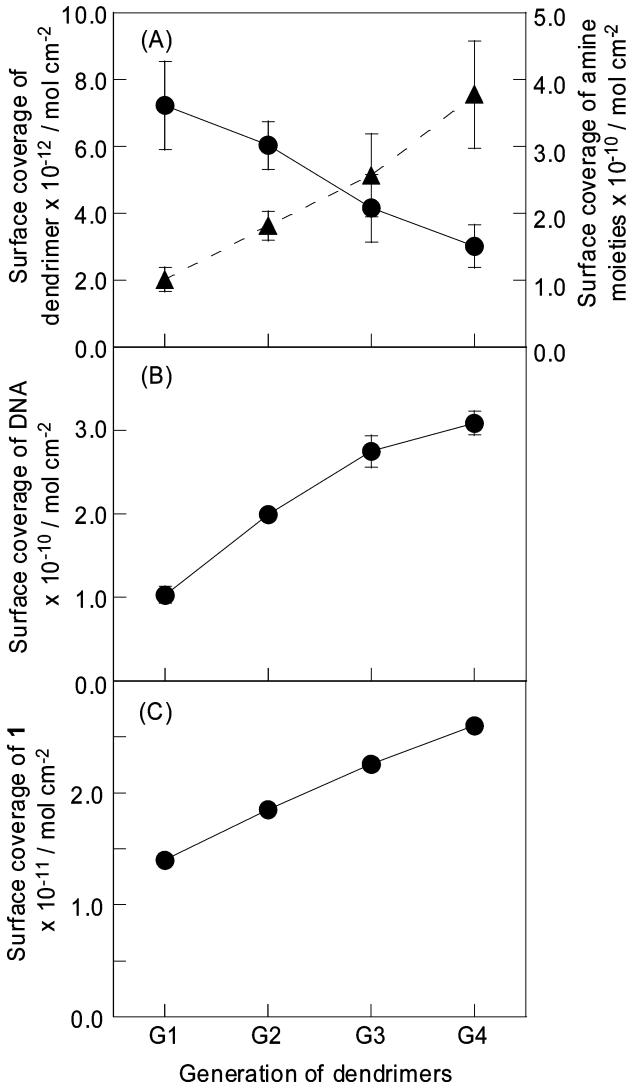

Figure 1. Surface coverages of (A) dendrimers (solid line) and amino moieties (dashed line), (B) DNA, and (C) **1** on an ITO electrode.

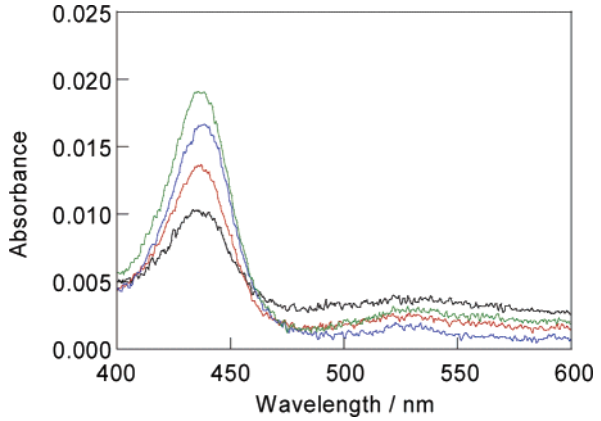

Figure 2. Electronic absorption spectra of the (a) **G1**−DNA−**1**, (b) **G2**−DNA−**1**, (c) **G3**−DNA−**1**, and (d) **G4**−DNA−**1** systems on an ITO electrode.

upon increasing the generation of the dendrimer as a result of **1** being positioned further from the electrode and, therefore, unable to transmit electrons effectively to the ITO. If the dendrimers were not spherical but instead squashed onto the ITO electrodes, as described previously,[16] the thicknesses of the dendrimer layers on the ITO electrodes

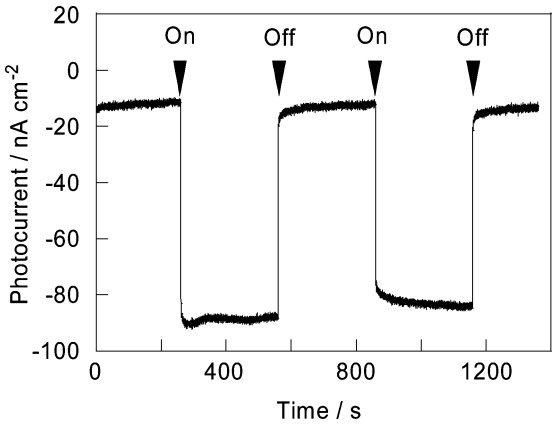

Figure 3. Photoelectrochemical responses of the **G4**−DNA−**1** system on an ITO electrode; illumination, 440 nm; electrolyte, Ar-saturated 0.1 M Na_2SO_4 solution containing 0.05 M TEOA; input power, 1 mW cm^{-2}; electrode radius, 3 mm; applied potential, 0.4 V vs Ag/AgCl.

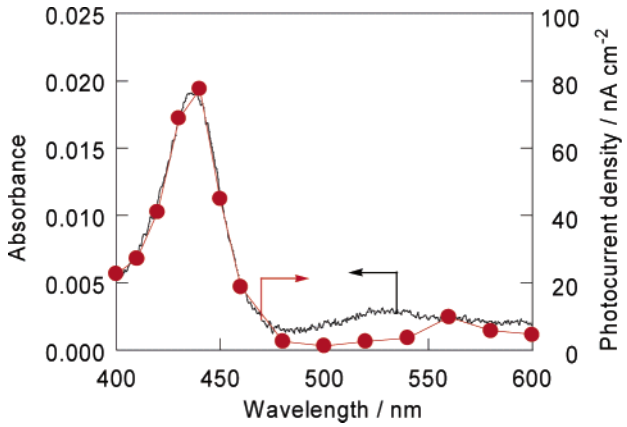

Figure 4. Electronic absorption spectrum (black line) and action spectrum (red line, closed circles) of the **G4**−DNA−**1** system on an ITO electrode; illumination, 440 nm; input power, 1 mW cm^{-2}; applied potential, 0.4 V vs Ag/AgCl; 0.1 M Na_2SO_4 solution containing 0.05 M TEOA.

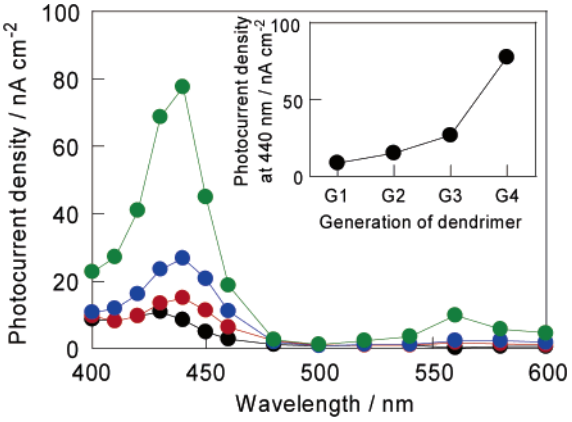

Figure 5. Action spectra of the **G1**−DNA−**1** (black), **G2**−DNA−**1** (red), **G3**−DNA−**1** (blue), and **G4**−DNA−**1** (green) systems on an ITO electrode; input power, 1 mW cm^{-2}; applied potential, 0.4 V vs Ag/AgCl; 0.1 M Na_2SO_4 solution containing 0.05 M TEOA. The inset displays a plot of the photocurrent at 440 nm vs the generation of the dendrimer.

should have been similar among each of the generations of dendrimers. The exponential growth of the photocurrent cannot be explained completely, however, by the squashing of dendrimers and the increased surface coverage of **1**. We suggest two explanations for the positive dendritic effect: (i) a higher-generation dendrimer has a higher surface coverage of amino moieties (see the Supporting Information,

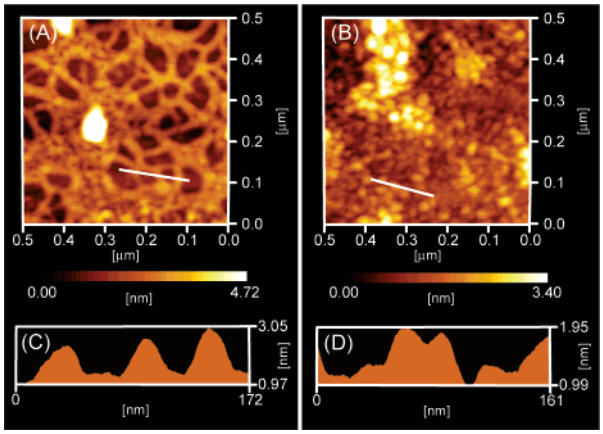

Figure 6. AFM images of the (A) **G1**−DNA and (B) **G4**−DNA films on mica. Height profiles of the (C) **G1**−DNA and (D) **G4**−DNA films.

Table S1), and thus these amino moieties act as sacrificial reagents more effectively than does TEOA; (ii) the average distance between the electrode and **1** was shorter in the higher-generation dendrimer because of multipoint interactions between the dendrimer and the DNA−**1** layer. If explanation (i) is correct, the photocurrent should not decrease in the absence of TEOA, because the photocurrent density for **G4**−DNA−**1** clearly decreased from 77.5 nA cm^{-2} in the presence of TEOA to 2.5 nA cm^{-2} in its absence (see the Supporting Information, Figure S2). However, we can rule out this explanation. If explanation (ii) is correct and **1** existed closer to the electrode surface, the DNA moieties would become more difficult to remove from the ITO electrodes at higher generations of the dendrimer. Atomic force microscopy (AFM) facilitated visualization of the surface topographic features of the dendrimer−DNA composite films and provided information regarding the positive dendritic effect. Images A and B of Figure 6 display AFM images of the **G1**−DNA and **G4**−DNA films assembled on a mica substrate. The surface coverage of the **G4**−DNA film was higher than that of the **G1**−DNA film; this observation is consistent with our previous finding that the surface coverages of the dendrimers and DNA increased upon increasing the generation of the dendrimer. The structure of the **G4**−DNA film formed on a mica surface is different from that of the **G1**−DNA film. However, the structural difference did not bring about the different microenvironments of porphyrin **1** in all electrodes because all electrodes coated with **G1**-DNA-**1**, **G2**-DNA-**1**, **G3**-DNA-**1**, and **G4**-DNA-**1** exhibited an identical absorption maximum at 436 nm, as shown in Figure 2. We expected, therefore, that rather than the structural differences, the different distances between porphyrin and the electrode are important for the positive dendritic effect. In practice, the film thickness (ca. 2 nm) of the **G4**−DNA film on the mica surface was less than that (ca. 3 nm) of the **G1**−DNA film (panels C and D of Figure 6). We attribute the higher surface coverage of the thin film of the **G4**−DNA film to **G4** more tightly adsorbing DNA through multipoint interactions, as indicated in Figure 7. We estimated the quantum yields of the **G1**−DNA−**1**, **G2**−DNA−**1**, **G3**−DNA−**1**, and **G4**−DNA−**1** systems to be 0.2, 0.3, 0.4, and 1.0%, respectively (at 440 nm and a 0.4 V bias voltage; see Figure S3 and Table S4 of the Supporting Information).

In comparison, the photocurrent density of a poly(allylamine hydrochloride) (**PAH**)−DNA−**1** membrane displayed a photoelectrochemical response (14 nA cm^{-2} at 440 nm and 0.4 V bias voltage) 5.6 times smaller than that of the **G4**−DNA−**1** membrane (see the Supporting Information, Figure S4b). In view of our observation that the photocurrent response could be repeated reversibly, it is unlikely that the **PAH** membrane peeled off the ITO electrode. Because the surface coverages of **1** were nearly identical for the **PAH**−DNA−**1** and **G4**−DNA−**1** membranes (2.8×10^{-11} and 2.6×10^{-11} mol cm^{-2}, respectively; see the Supporting Information, Figure S4a), the low photocurrent density of the former may suggest that the **PAH**, which adsorbed onto the ITO electrode in one dimension, did not interact as strongly with DNA as did the dendrimer, which adsorbed in two dimensions.

Furthermore, to show the importance of DNA in this system, the porphyrin **1** was adsorbed onto the PAMAM surface using poly(vinylsulfonic acid)potassium salt (**PVS**) as a dye matrix instead of DNA. The photocurrent density of a **G4**−**PVS**−**1** membrane displayed a photoelectrochemical response (21 nA cm^{-2} at 440 nm and 0.4 V bias voltage) that was less than one-fourth that of the **G4**−DNA−**1** membrane (77.5 nA cm^{-2} at 440 nm and 0.4 V bias voltage; see the Supporting Information, Figure S5). The reason remains unclear. We expect that the higher photoelectrochemical response of the **G4**−DNA−**1** membrane was achieved by suppression of self-quenching of porphyrin **1** intercalated in DNA.[4c,17]

Conclusions

Our studies have revealed that PAMAM dendrimers can be used as stationary phases upon which commercial cationic porphyrin **1** intercalated in DNA may be deposited onto an ITO electrode. The dendrimer−DNA−porphyrin membranes were readily prepared and stable under the conditions employed. The resulting electrodes generated photocurrents in irradiation with visible light; indeed, the photocurrent densities increased exponentially upon increasing the generation of the dendrimer, i.e., we observed a positive dendritic effect in these systems. We believe that the main reason for this positive dendritic effect is that relatively strong electrostatic interactions exist between the DNA and the higher-generation dendrimers, leading to tight adsorption of the porphyrin. Nevertheless, the values of the photocurrents and

(16) The mean dendrimer height on a mica surface was measured using atomic force microscopy (AFM) and the particle profiles, as outlined previously (see: Li, J.; Piehler, L. T.; Qin, D.; Baker, J. R., Jr.; Tomalia D. A.; Meier, D. J. *Langmuir* **2000**, *16*, 5613−5616). The height from **G5** to **G8** increased slowly upon increasing the generation. Each height was less than 2 nm and always smaller than the measured diameter, indicating that the dendrimer molecules on the mica surface were no longer spherical but instead dome-shaped. Because the height of **G5** was less than 1 nm, we believe that the heights of **G1**-**G4** on the ITO electrodes were also less than 1 nm.

(17) Konishi, T.; Ikeda, A.; Asai, M.; Hatano, T.; Shinkai, S.; Fujitsuka, M.; Ito, O.; Tsuchiya, Y.; Kikuchi, J. *J. Phys. Chem. B* **2003**, *107*, 11261−11266.

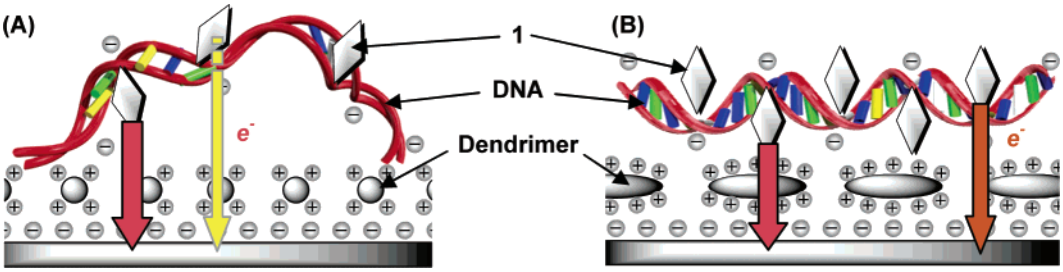

Figure 7. Schematic illustrations of (A) low-generation-dendrimer−DNA−**1** and (B) high-generation-dendrimer−DNA−**1** films. Arrows indicate the transmission of electron from **1** to the ITO electrode. When **1** is positioned near to the ITO electrode, it can transmit electrons (orange arrows), but when it is further away from the electrode, it cannot do so (yellow arrow).

the quantum yields remained low; we hope to improve these drawbacks in future studies. To do so, we might use dendrimers including an electron acceptor; alternatively, we might produce a mixture with titania nanoparticles (TiO_2).

Experimental Section

Materials. Calf thymus DNA (ctDNA) and the PAMAM dendrimers **G1**−**G4** were purchased from Sigma-Aldrich Chemical Co., Inc., and Aldrich Chemical Co., Inc., respectively. Compounds **1**, **PAH** (M_w = 10 000), and **PVS** (M_w = 30 000) were purchased from Tokyo Kasei Kogyo Co., Ltd., Nitto Boseki Co., Ltd., and Wako, respectively. 2,2′,2″-Nitrilotriethanol (TEOA) was purchased from Kanto Chemical Co., Inc.

Preparation of ITO Electrodes with Modified DNA and Porphyrin. A 3-mercaptopropionic acid-covered ITO electrode possessing an anionic surface[18] was exposed to a 0.1 M phosphate buffer (pH 7.0) containing cationic dendrimers (**G1**−**G4**, 1.0 mM) for 15 min. After being washed with water and dried under a stream of nitrogen, the electrode was immersed in a 0.1 M phosphate buffer (pH 7.0) containing DNA (0.59 mM in nucleotide phosphate)[19] for 15 min. After being washed with water and dried under a stream of nitrogen, the DNA-deposited electrode was immersed in a 0.1 M phosphate buffer (pH 7.0) containing **1** (1.0 mM). After 15 min, the electrode was washed with water and dried under a stream of nitrogen. The ITO electrodes presenting the deposited **PAH**−DNA−**1**, **G1**−**PVS**−**1**, and **G4**−**PVS**−**1** membranes were also prepared using a similar method.

UV−**Vis Absorption Spectra.** UV−vis spectra were recorded using a UV-2550PC spectrometer (Shimadzu Corp.). Experiments were performed at room temperature directly on the ITO electrodes modified with **G1**−DNA−**1**, **G2**−DNA−**1**, **G3**−DNA−**1**, and **G4**−DNA−**1** membranes.

QCM Measurements. The adsorptions of **G1**−**G4**, DNA, and **1** in phosphate buffer were monitored using a quartz crystal microbalance (QCM; USI system). The QCM employed was a crystal of a commercially available 9-MHz, AT-cut quartz plate on which Au electrodes were deposited on both sides (area: 0.16 ± 0.01 cm^2). Electrodes on the QCM plate were connected to a handmade oscillator, which normalized the value of ΔF (Hz) to the weight W (ng cm^{-2}). The frequency changes were monitored every 10 s using a universal frequency counter (Iwatsu Co., Japan, Model SC 7201). The dendrimer−DNA−**1**-deposited QCM resonators were prepared in a manner similar to that described for the preparation of the dendrimers−DNA−**1**-deposited ITO electrode. The frequency changes of the quartz crystals were measured in air after each modification step.[20] All of the measurements were performed under an argon atmosphere at room temperature.

Photoelectrochemical Measurements. A 500 W Xe-arc lamp (UI-502Q; Ushio, Inc.) was used as the light source in the photoelectrochemical studies; a monochromator (SPG 120S; Shimadzu Corp.) was used to obtain different wavelengths. The light intensity was measured using an energy and power meter (TQ8210; Advantest Corp.). Photocurrents were measured in 0.1 M aqueous Na_2SO_4 solution using a three-electrode photoelectrochemical cell consisting of the modified ITO electrode. All measurements were performed in the presence of TEOA (0.05 M) as a sacrificial reagent under an argon atmosphere.

AFM Measurements. AFM images were recorded using an SPI-3800N System from Seiko Instruments Inc., Japan, in the tapping mode with a 20 m scanner. For AFM observations, a mica plate was chosen as a substrate for the alternate layer-by-layer assembly; it was analyzed immediately after cleavage under a clean atmosphere.[11]

Acknowledgment. We thank Mr. H. Horiuchi for his skill in preparing the specially designed glass cells. This study was supported by Grants-in-Aid for Scientific Research from the Ministry of Education, Science and Culture of Japan.

Supporting Information Available: Supporting Tables (S1−S4) and Figures (S1−S4). This material is available free of charge via the Internet at http://pubs.acs.org.

CM061812I

(18) Yan, C.; Zharnikov, M.; Gölzhäuser, A; Grunze, M. *Langmuir* **2000**, *16*, 6208−6215.

(19) The concentration of the stock solution of ctDNA (0.59 mM in nucleotide phosphate, NP) was determined from the UV absorbance at 260 nm using a molar extinction coefficient of 6.6×10^3 M^{-1} cm^{-1} per nucleotide phosphate. See: Felsenfeld, G.; Hirschman, S. Z. *J. Mol. Biol.* **1965**, *13*, 407−427.

(20) (a) Sauerbrey, G. *Z. Phys.* **1959**, *155*, 206−222. (b) Caruso, F.; Serizawa, T.; Furlong, D. N.; Okahata, Y. *Langmuir* **1995**, *11*, 1546−1552. (c) Lvov, Y. In *Protein Architecture: Interfacing Molecular Assemblies and Immobilization Biotechnology*; Lvov, Y., Möhwald, H., Eds.; Marcel Dekker: New York, 2000; p 125. (d) Ebara, Y.; Okahata, Y. *J. Am. Chem. Soc.* **1994**, *116*, 11209−11212. (e) Ebara, Y.; Itakura, K.; Okahata, Y. *Langmuir* **1996**, *12*, 5165−5170.